Zn-doping effect on the energy barrier to magnetization reversal in superparamagnetic nickel ferrite nanoparticles

José Trinidad Elizalde Galindo, Cristian E. Botez, Luis Fuentes Cobas, José Andrés Matutes Aquino

Abstract

Measurements of ac-susceptibility and dc-magnetization were carried out on samples of $Ni_{1-x}Zn_xFe_2O_4$ nanoparticles (x = 0, 0.25, 0.5, 0.75) with average diameters <D> ≈ 7 nm. Values of the superparamagnetic blocking temperature ***T***B were obtained from the characteristic temperature behavior of the imaginary susceptibility $\chi_{imag.}$ An Arrhenius-type law, which accurately describes the relationship between the observation time τ_{obs} and the blocking temperature, was used to determine the effective energy barrier to magnetization reversal U_{eff}. A Zn-content dependence of the energy barrier is observed, where Ueff changes little for $0 \leq x \leq 0.25$, it peaks at x = 0.5, and decreases back upon further Zn-doping. The large increase of U_{eff} at x = 0.5 is attributed to an enhanced magnetic anisotropy induced by the crossover between two spatial arrangements of spins in the A and B sub-lattices of the ferrimagnetic inverse spinel.

Introduction

The relaxation time of an ideal system of noninteracting, single-domain, and monodisperse ferromagnetic nanoparticles that have uniaxial magnetic anisotropy is

given by the Néel–Brown equation [1],

$$\tau = \tau_0 \exp\left(\frac{K_u V}{k_B T}\right), \qquad (1)$$

which describes how rapidly the magnetic moment of each particle flips along an easy axis by thermal activation. Here τ_0 is a time constant, k_B is the Boltzman constant, T is the absolute temperature, and K_uV is the energy barrier between the parallel and anti-parallel easy directions (with Ku being the magnetic anisotropy constant and V the volume of each particle). At a given temperature, measurements performed on such a system over an observation time τ_{obs} show ferromagnetic properties only if $\tau_{obs} << \tau$. For $\tau_{obs} >> \tau$, the nanoparticle assembly exhibits paramagnetic behavior, a phenomenon often referred to as superparamagnetic relaxation. By setting $\tau = \tau_{obs}$ in (1) a superparamagnetic blocking temperature $T_B = K_uV/k_B \ln(\tau_{obs}/\tau_o)$ can be defined. Accordingly, the system is in a “blocked” ferromagnetic state for T << TB, but becomes (super) paramagnetic for T >> T_B. In a real system the particles are not monodispersed monodispersed, but exhibit a distribution of volumes and, correspondingly, a distribution of blocking temperatures that has an average *T*B. Such a system also possesses an effective energy barrier to magnetization reversal U_{eff} [2], whose value depends not only on the distribution of the particle volumes, but also on the relaxation mechanism and on the type and strength of the inter-cluster magnetic interactions. U_{eff} strongly affects physical quantities that are essential for technological applications, such as the energy loses in high-permeability inductors and wave absorbers [3] or the heating power in ferrofluids formedical hyperthermia [4].Consequently, the experimental determination of the effective energy barrier to magnetization reversal is important in at least two

respects. First, it provides a means of validating physical models aimed at describing the superparamagnetic relaxation (by comparing the predictions from such models with the measured values of U_{eff}). Second, accurate determinations of U_{eff} for nanoparticle assemblies prepared under different conditions and/or having different chemical compositions, offer excellent opportunities to understand, and possibly control, the effect of various synthesis parameters on the magnitude of the energy barrier to magnetization reversal and other key magnetic quantities.

Previous studies have suggested that the Arrhenius-type relaxation described by (1) is not restricted to an ideal system of magnetic nanoparticles, but might carry over to more general cases, including systems where the particle interactions cannot be neglected [5], or systems where relaxation is measured in a constant external magnetic field [6]. A general expression for this behavior can be written as

$$\tau_{obs} = \tau_0 \exp\left(\frac{U_{eff}}{k_B \overline{T}_B}\right) . \qquad (2)$$

Should (2) hold for a particular system, one could (in principle) use it to experimentally determine the energy barrier to magnetization reversal U_{eff} through measurements of the average blocking temperature T_B carried out over different observation times τ_{obs}. Choosing how to measure T_B, however, is not always straightforward. Often [6, 7], T_B is obtained from the maximum of the dc-magnetization measured after cooling the sample in zero field (ZFC). Yet, besides neglecting non-linear effects in the equilibrium magnetization [8], this approach has limited usefulness for testing the validity of (2) as, for dc-measurements, τ_{obs} cannot be varied over a wide

enough range of values. However, acsusceptibility measurements of T_B can be carried out at different frequencies (observation times) whose values extend over several orders of magnitude, allowing one to first confirm the relaxation behavior described by (2) and then to use it to determine U_{eff}. Either the real or the imaginary part of the ac-susceptibility can be used to determine T_B [2, 9].

Here we report ac-susceptibility measurements aimed at uncovering the dependence of the energy barrier to magnetization reversal U_{eff} on the Zn-content *x* for assemblies of $Ni_{1-x}Zn_xFe_2O_4$ nanoparticles with $0 \leq x \leq 0.75$. We chose this particular system as previous studies [10] have indicated that adding Zn^{2+} ions to bulk spinel ferrites has a strong effect on their magnetic properties, although Zn2+ ions are non-magnetic. Should this effect carry over to nanoparticles, Zn-doping might be used to control properties that are specific to nano-sized magnetic systems such as the superparamagnetic relaxation. Our data shows that the magnitude of the energy barrier to magnetization reversal is indeed dependent on the Zn content, exhibiting a notable enhancement when half of the magnetic Ni^{2+} ions are replaced with diamagnetic Zn^{2+} (x = 0.5). We attribute this behavior to the magnetocrystalline changes that occur upon Zn doping.

Experimental procedure

$Ni_{1-x}Zn_xFe_2O_4$ nanoparticles (x = 0, 0.25, 0.5, 0.75) were prepared by the co-precipitation method. $Ni(NO_3)_2 \cdot 6H_2O$, $Zn(NO_3)_2 \cdot 6H_2O$ and $FeCl_3 \cdot 6H_2O$ were dissolved into distilled water at room temperature with an NaOH solution added as precipitating agent. A 1 h digestion step at 90 °C was carried out to crystallize the

phases. Eventually, the precipitated particles were thoroughlywashed and dried at 60 °C.

Synchrotron X-ray powder diffraction measurements were performed on the X7B beamline at the National Synchrotron Light Source (Brookhaven National Laboratory). X-rays of wavelength 0.922 Å were selected by a double flatcrystal monochromator and a Mar345 flat image plate was used to detect the diffracted beam. Diffraction images were collected using an exposure time of 60 s. Finally, the images were processed by integrating over the projections of the Debye–Scherrer cones onto the flat detector using the Plot2D software [11].

Magnetization experiments were carried out using a Quantum Design Physical Property Measurement System (PPMS). The ac-susceptibility was measured upon heating in steps of 2.5K, from 3 to 298 K. At each temperature step the imaginary part of the susceptibility χimag was recorded for five frequencies (100, 500, 1000, 5000, and 10 000Hz) in an oscillating magnetic field of amplitude 3Oe. The dc-magnetization was measured as a function of the applied magnetic field (for -70 kOe ≤ H ≤ 70 kOe), at four temperatures: 3, 6, 60 and 295 K. Before each set of measurements was taken the magnetometer was calibrated using a palladium standard.

Results and discussion

Figure 1 shows the synchrotron X-ray diffraction data from a system of $Ni_{0.25}Zn_{0.75}Fe_2O_4$ nanoparticles (the inset shows the corresponding diffraction image). All peaks could be indexed to the standard pattern of Ni-Zn ferrite (PDF # 08-0234), indicating that no impurities were present in the sample. The average particle size was determined from the full width at half maximum (FWHM) of the (440) peak using the

Scherrer equation [12], where the FWHM was obtained from the best fit of the peak profile to a combination of Gaussian and Lorentzian functions. The same procedure was applied to the other three $Ni_{1-x}Zn_xFe_2O_4$ samples (x = 0, 0.25, 0.5) and it was found that the average particle size for the systems used in this study was <D> = 7±3 nm.

The open symbols in Fig. 2a represent the temperature dependence of the imaginary component of the acsusceptibility χ_{imag} measured on an assembly of $Ni_{0.25}Zn_{0.75}$ Fe_2O_4 nanoparticles. Each of the five curves corresponds to a different measurement frequency *v* or, equivalently, to an observation time τ_{obs} = 1/v. The data show that χ_{imag} initially increases with increasing T, reaches a maximum at T = T_B, and eventually decreases upon further heating. This behavior is indicative of the progressive unblocking of the particles magnetic moment as the system goes into the superparamagnetic state. For each observation time/frequency the average blocking temperature T_B was determined from fits to the "χimag vs. *T*" dependence of a fourth-order polynomial (solid curves). As expected, TB was found to shift towards larger values as the observation time was decreased. This behavior is detailed in Fig. 2b where the natural logarithm of τ_{obs} is represented vs. the inverse blocking temperature (filled squares).

The solid line here is the best fit of (2) with the effective energy barrier to magnetization reversal Ueff and the time constant τ_0 as variable parameters. The best fit demonstrates that the "T_B vs. τ_{obs}" dependence is excellently described by an Arrhenius-type relaxation law for a broad range of observation times, and yields U_{eff} = 0.12 eV and $\tau_0 = 8\times10^{-11}$ s. Similar ac-susceptibility measurements and analysis were

carried out for $Ni_{1-x}Zn_xFe_2O_4$ samples with a different Zn content (x = 0, 0.25 and 0.5) and the corresponding U_{eff} values were determined.

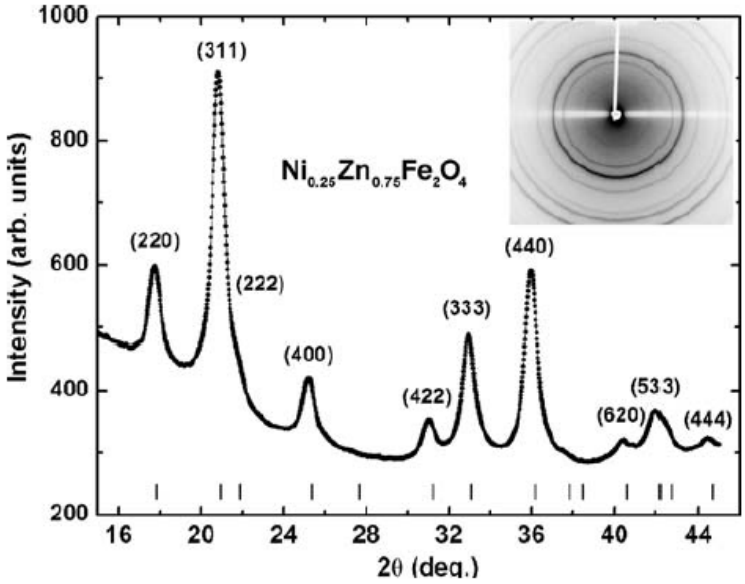

FIGURE 1 Synchrotron X-ray powder diffraction pattern from $Ni_{0.25}Zn_{0.75}Fe_2O_4$ nanoparticles. The *vertical bars* indicate the 2θ positions of the (hkl) Bragg reflections. The *inset* shows the projection of the Debye–Scherrer cones onto the flat plate detector

The Zn-content dependence of the energy barrier to magnetization reversal, obtained from fits of (2) to the acsusceptibility data, is shown in Fig. 3a. We observe that U_{eff} changes little when the Zn content x is increased from 0 to 0.25, but exhibits a pronounced maximum at x = 0.5. Upon further Zn-doping (to x = 0.75) lower Ueff values reenter. As expected, TB (measured at 100 Hz) displays a similar behavior: as shown in Fig. 3b, $T_B \approx 40$ K for $x \leq 0.25$, it increases steeply to reach 182.5K for x = 0.5, and decreases back to about 80 K for x = 0.75. In essence, we observe that two key quantities related to the superparamagnetic relaxation of a system of nickel-zinc ferrite nanoparticles system, U_{eff} and TB, are strongly enhanced when the Zn content has the particular value x = 0.5. We will focus our discussion below on the behavior of the

energy barrier to magnetization reversal. To propose an explanation for the abrupt increase of U_{eff} at x = 0.5 it is necessary to consider the microscopic details of doping Zn into the structure of inverse spinel ferrites, and its effect on themacroscopicmagnetic properties of these materials. It iswell established thatwhen adding Zn to bulk $NiFe_2O_4$ to obtain $Ni_{1-x}ZnxFe_2O_4$, the Zn^{2+} ions have a strong preference for the tetrahedral (A) sites [13]. This yields the general formula $Zn_x^{2+}Fe_{1-x}^{3+}\left[Ni_{1-x}^{2+}Fe_{1+x}^{3+}\right]O_4$ for the mixed Zn-Ni ferrite, where the cations within the brackets are located at octahedral (B) sites.

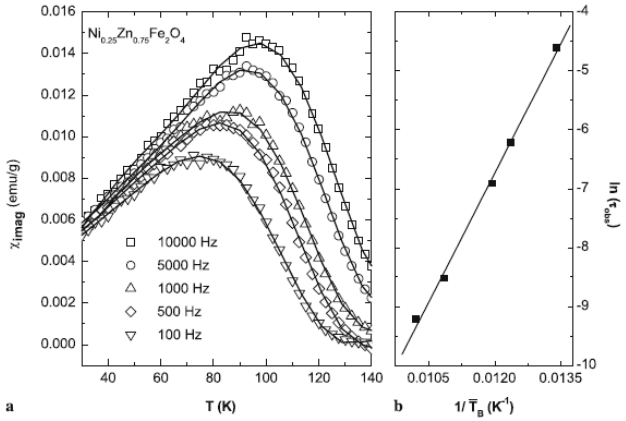

FIGURE 2 (**a**) Imaginary component of the ac-susceptibility of an assembly of $Ni_{0.25}Zn_{0.75}Fe_2O_4$ nanoparticles as a function of temperature at different frequencies/observation times (*open symbols*). The *solid lines* represent best fits (to a polynomial function) that allow the determination of the average blocking temperature T_B for each observation time τ_{obs}. (**b**) $\ln(\tau_{obs})$ vs. $1/T_B$ data (*filled squares*) and best fit to (2) (*solid line*)

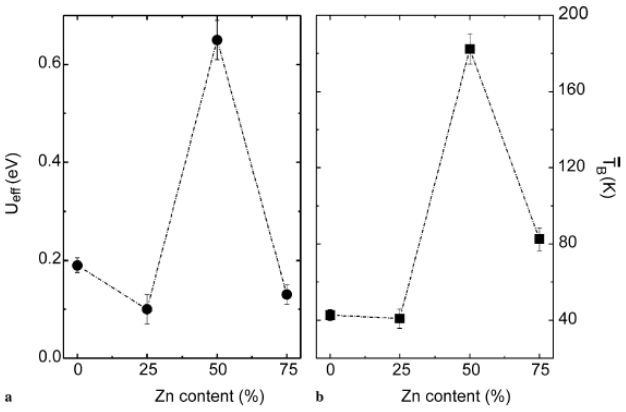

FIGURE 3 Zn-content dependence of (**a**) the effective energy barrier to magnetization reversal U_{eff} and (**b**) the average blocking temperature T_B (measured at 100 Hz) for $Ni_{1-x}Zn_xFe_2O_4$ nanoparticles

Interestingly, this cation distribution leads to two competing effects on the netmagnetic moment.Adding diamagnetic Zn^{2+} decreases the magnetic moment of the A lattice, and, consequently, contributes to the increase of the net moment of the

ferrimagnetic spinel with increasing x. At the same time, Zn incorporation reduces the number of Fe^{3+} ions on A sites, which, in turn, weakens the superexchange interaction between the A and B sublattices and tends to decrease the net magnetic moment with increasing x. Experiments [10] have shown that the former effect is more pronounced at low Zn-content values, whereas the latter dominates at higher values of x with a crossover value of $x \approx 0.5$, which is exactly the Zn-content where we observed a steep increase of U_{eff}. In addition, it was found that for Zn-content values below 0.5 the tetrahedral (A) and octahedral (B) site Fe^{3+} moments have a near collinear arrangement, whereas above 0.5 the molecular field of the B sublattice assumes increasing importance, and consequently a triangular or antiferromagnetic spin arrangement of the B sites arises. This change in the spatial arrangement of the Fe3+ ions is likely to enhance the magnetic anisotropy (and U_{eff}) in the vicinity of the crossover point ($x = 0.5$), consistent with the observation of a slight increase in the low-temperature coercivity with the increasing Zn-content between $x = 0$ and $x = 0.5$. Upon further doping, lower values of the energy barrier to magnetization reversal reenter as the spin dilution in the B-sublattice intensifies. It is important to note that the analysis above is based on the assumption that the Zn^{2+} ions are predominantly incorporated into tetrahedral (A) sites. Although this cation distribution has been convincingly demonstrated for bulk Ni-Zn ferrites, it does not necessarily carry over to Ni-Zn ferrite nanoparticles. Indeed, recent studies [14, 15] have reported that certain methods of nanoparticle preparation may lead to a different cation arrangement, where Zn^{2+} ions are present (and have significant occupancies) in the B sites. A proposed signature of this distribution is a drastically reduced value of the maximum magnetization at

temperatures below the blocking temperature. For example, Morrison et al. [14] observed that Zn-incorporation into Bsites of nanoparticles with a Zn-content x = 0.44 (cation distribution confirmed by extended X-ray absorption fine structure spectroscopy) led to a maximum magnetization σ_{max} (at T = 10 K and 30 kOe) whose value was only 32% of that measured for the bulk material. Other studies [16], however, reported the synthesis of $Ni_{1-x}Zn_xFe_2O_4$ nanoparticles where the Zn^{2+} ions almost exclusively incorporate into A sites (as they do in the bulk). This distribution was observed to lead to 1. a σ_{max} value (at T=5K, x = 0.5, and 50 kOe) almost 75% of its bulk counterpart, and 2. a "σ_{max} vs. x" dependence that closely resembles the one for the bulk (where σ_{max} increases with increasing x for x < 0.5, but decreases back upon further Zn doping).

In order to determine which of the two above-described cation arrangements applies to the Ni-Zn ferrite nanoparticles used in the present study we measured their temperature and Zncontent dependence of the maximum magnetization. Figure 4 shows the magnetization vs. applied magnetic field curves recorded at four different temperatures (3, 6, 60 and 295 K) for nanostructured $Ni_{0.5}Zn_{0.5}Fe_2O_4$.

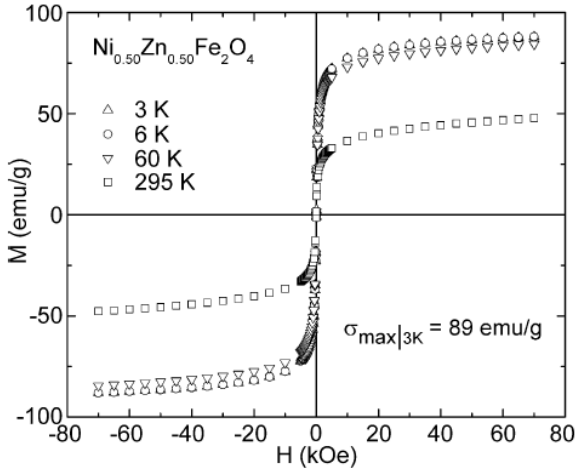

FIGURE 4 Magnetization dependence on the applied magnetic field at different temperatures for $Ni_{0.5}Zn_{0.5}Fe_2O_4$ nanoparticles

As expected for a system of magnetic nanoparticles the magnetization does not saturate, but reaches a maximum value σ_{max} for the maximum applied field of 70 kOe. σ_{max} is temperature dependent: it considerably increases, from 48 to 84 emu/g, as the temperature is lowered from 295 K to 60 K and changes little, from 84 to 89 emu/g, upon further cooling to 3K. The value of the maximum magnetization at 3K, $\sigma_{max}|3\ K$ = 89 emu/g, is 74.7% of its bulk counterpart (119 emu/g), in excellent agreement with the above-mentioned observations of Ychiyanagy et al. [16].

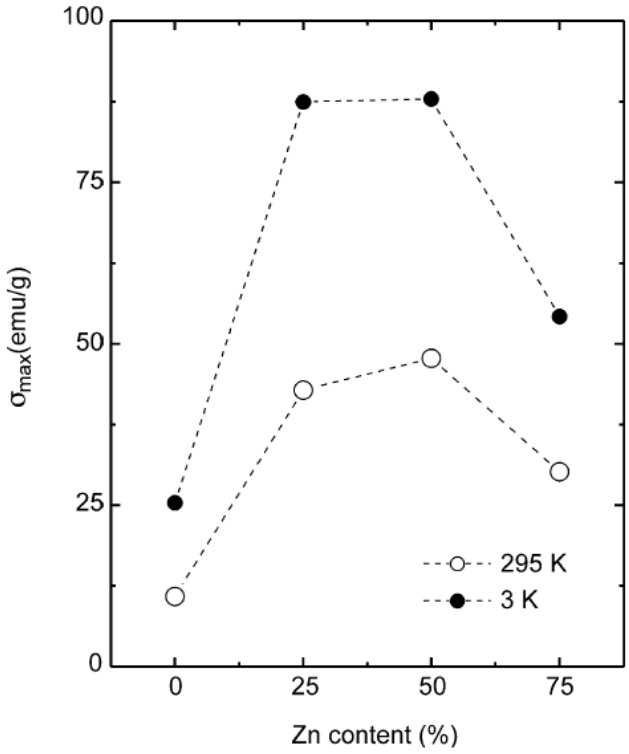

FIGURE 5 Maximum magnetization σ_{max} vs. Zn content x for $Ni_{1-x}Zn_xFe_2O_4$ nanoparticles at 295 K (○) and at $T = 3$ K (●)

This strongly suggests that the Zn^{2+} ions in our Zn- Ni ferrite samples are predominantly incorporated into tetrahedral A sites. Further confirmation of this cation distribution comes from the results for the Zn-content dependence of the maximum magnetization shown in Fig. 5. Here, the net σ_{max} increases with increasing x for x < 0.5,

indicating that the moment of the A sublattice is gradually reduced by the incorporation of diamagnetic Zn. Also, σmax decreases for x > 0.5, as doping more Zn atoms into the tetrahedral sites weakens the superexchange interaction between sub-lattices A and B by reducing the Fe^{3+} occupancy in the A sublattice and by destroying the collinearity of the tetrahedral and octahedral Fe^{3+} moments.

Summary

We have investigated the effect of Zn-doping on the superparamagnetic relaxation of nanosized nickel ferrite particles. Our temperature-resolved ac-susceptibility data demonstrates that the relaxation of these systems is well described by an Arrhenius-type law, a behavior which allows a precise determination of the effective energy barrier to magnetization reversal U_{eff}. We observe that the Zn-content dependence of U_{eff} exhibits a pronounced maximum when half of the magnetic Ni^{2+} ions are replaced by nonmagnetic Zn^{2+}. The average blocking temperature T_B, measured at a given frequency, shows a similar behavior. The observed increase of U_{eff} is attributed to an enhanced magnetic anisotropy induced by the crossover between two magnetocrystalline regimes. Our findings demonstrate the ability to control the superparamagnetic relaxation of ferrimagnetic spinel nanoparticles through chemical manipulations.

Acknowledgements

JTEG, AHA and CEB would like to acknowledge support from the University of Texas Research Fund. Use of the National Synchrotron Light Source, Brookhaven National Laboratory, was supported by the U.S. Department of Energy, Office of Basic Energy Sciences, under contract number DE-AC02-98CH10886.

References

1 L.Néel, Ann. Geophys. (C.N.R.S.) **5**, 99 (1949)

2 F. Luis, E. del Barco, J.M. Hernandez, E. Remiro, J. Bartolome, J. Tejada, Phys. Rev. B **59**, 11 837 (1999)

3 T. Tsutaoka, J. Appl. Phys. **93**, 2789 (2003)

4 R.E. Rosenweig, J. Magn. Magn. Mater. **252**, 370 (2002)

5 R.D. Zysler, D. Fiorani, A.M. Testa, J. Magn. Magn. Mater. **224**, 5 (2001)

6 Y.D. Zhang, J.I. Budnick, W.A. Hines, C.L. Chen, J.Q. Xiao, Appl. Phys. Lett. **72**, 2053 (1998)

7 W. Luo, S.R. Nagel, T.F. Rosenbaum, R.E. Rosenweig, Phys. Rev. Lett. **67**, 2721 (1991)

8 M. Hanson, C. Johansson, S. Mørup, Phys. Rev. Lett. **81**, 735 (1998)

9 F. Luis, F. Petroff, J. Bartolom´e, J. Phys.: Condens. Matter **16**, 5109 (2004)

10 E.W. Gorter, Nature **165**, 798 (1950)

11 A.P. Hammersley, S.O. Svenson, M. Hanfland, A.N. Fitch, D. Hauserman, High Press. Res. **14**, 235 (1996)

12 B.D. Culity, *Elements of X-ray Diffraction*, 2nd edn. (Addison-Wesley, New York, 1978), pp. 101–102

13 E.W. Gorter, Philips Res. Rep. **9**, 295 (1954)

14 S.A. Morrison, C.L. Cahill, E.E. Carpenter, S. Calvin, R. Swaminathan, M.E. McHenry, V.G. Harris, J. Appl. Phys. **95**, 6392 (2004)

15 N. Ponpandian, A. Narayansamy, C.N. Chinnasamy, N. Sivakumar, J.M. Greneche, K. Chattopadhyay, K. Shinoda, B. Jeyadevan, K. Tohji, Appl. Phys. Lett. **86**, 192 510 (2005)

16 Y. Ichiyanagi, T. Uehashi, S. Yamada, Phys. Stat. Solidi **1**, 3485 (2004)